Atomic and electronic structure of the CdTe(001) surface: LDA and *GW* calculations

S. Gundel
Physikalisches Institut, Experimentelle Physik III, Universität Würzburg, Am Hubland, D-97074 Würzburg, Germany

A. Fleszar
Institut für Theoretische Physik, Universität Würzburg, Am Hubland, D-97074 Würzburg, Germany

W. Faschinger
Physikalisches Institut, Experimentelle Physik III, Universität Würzburg, Am Hubland, D-97074 Würzburg, Germany

W. Hanke
Institut für Theoretische Physik, Universität Würzburg, Am Hubland, D-97074 Würzburg, Germany

(Received 24 November 1998)

The CdTe(001) surface has been studied theoretically by means of the local-density approximation (LDA) to the density-functional theory and the many-body *GW* approach. Within the LDA method the minimum-energy geometry is determined for several reconstruction models and a phase diagram of stable structures is established. For the most stable reconstruction model over a large range of ambient conditions, the $c(2\times2)$ Cd-vacancy reconstruction, the surface electronic structure has been determined by means of the analysis of the spatial behavior of Kohn-Sham orbitals and the local density of states. In addition, self-energy corrections to the energies of the surface states are determined using the *GW* method. The spin-orbit interaction, which is important in CdTe, is perturbatively included in calculations. [S0163-1829(99)06323-7]

I. INTRODUCTION

Recent success in the fabrication of optoelectronic devices on the basis of II-VI compounds has attracted renewed interest in these materials. The technological applicability relies on the preparation of well defined heterostructures, in which the quality of substrate and junction surfaces determines the characteristics of the device. The CdTe (and the similar $Cd_{0.96}Zn_{0.04}Te$) are often used as substrates for the growth of ternary II-VI semiconducting heterojunctions. In particular, the (001) growth orientation in the molecular beam epitaxy process is frequently applied. For these reasons, a knowledge of the physical properties of the CdTe(001) surface is of great importance.

Many new experimental studies of the CdTe(001) surface have been undertaken recently. Among surface-sensitive experimental techniques that have been applied are scanning tunneling microscopy,[1] grazing incidence x-ray diffraction,[2] reflection high-energy electron diffraction,[3,4,10,2] high-resolution transmission electron microscopy,[5] and high-resolution low-energy electron diffraction.[6] The electronic structure at the CdTe(001) surface was studied by angle-resolved photoelectron spectroscopy in the energy domain of valence bands,[7–9] x-ray photoelectron spectroscopy[10–12] in order to determine the surface core level shifts and surface composition,[3,10] and very recently, by reflection electron energy loss spectroscopy.[13]

As a result, the atomic structure of the CdTe(001) surface is experimentally well understood. For most preparation conditions, the most stable CdTe(001) surface under vacuum conditions is Cd terminated with a Cd coverage of 0.5 atomic layers. The dominant reconstruction pattern is either a $c(2\times2)$, or a mixed $c(2\times2)$ and (2×1) structure. Under special preparation conditions (high Te flux and low annealing temperature) a Te-terminated, (2×1) reconstruction is observed with a Te coverage of 1.5 monolayers.[14] This behavior resembles very much that of the ZnSe(001) surface, whose similar atomic structure has been experimentally determined[15,16] and confirmed by first principles, total energy calculations.[17,18] Therefore the polar (001) surfaces of a number of II-VI materials display a rather similar atomic structural behavior.

The aim of the present article is twofold. First, we would like to provide a theoretical verification of the above experimental findings for CdTe(001) via total energy calculations, in analogy to the work done on the ZnSe(001) surface.[17–19] The second goal is the study of the electronic structure of the $c(2\times2)$ reconstruction, which, according to both experiment and our calculations, is energetically the most stable surface over a large range of growth conditions. The study of the electronic structure, i.e., of the one-particle excitation spectrum in the system, requires in principle a complicated apparatus of many-body techniques. We shall therefore analyze in detail the electronic structure of the $c(2\times2)$ surface within the density-functional-theory–local-density-approximation (DFT-LDA) theory[20] and the *GW* approximation, calculating explicitly self-energy corrections to one-particle binding energies of surface states and resonances.[35]

In the next section technical information about our computational method will be briefly reviewed. Then, in Sec. III, results of the total energy calculations for CdTe surfaces with atomic positions optimized from self-consistently calculated forces will be presented. In Sec. IV, we will analyze the electronic excitation spectrum for the $c(2\times2)$ reconstruction model and present plots of the dispersion of surface states and resonances. This will be compared with experimental results.

II. COMPUTATIONAL METHOD

Calculations have been performed within the local-density approximation to the density-functional formalism.[20] The electron ion interaction has been modeled by *ab initio*, norm-conserving pseudopotentials. II-VI semiconductors are not easy subjects for the application of the pseudopotential concept, because cations from the group II^B (Zn, Cd, Hg) possess shallow ''semicore'' *d* states which, as shown by Wei and Zunger,[21] contribute to the chemistry of these compounds. This problem can partly be overcome by keeping the shallow *d* states of cations in the core, and including a nonlinear core correction in the exchange-correlation energy functional, as proposed by Louie, Froyen, and Cohen.[22] An additional difficulty, which cannot be ignored when studying the electronic structure of tellurides, is due to strong relativistic effects, which result in a large spin-orbit splitting on the order of $\sim$ 1 eV of the uppermost valence bands at the Γ point. For both these reasons we have probed several pseudopotentials generated according to specific demands of successive stages of our work.

The calculations of total energies were performed using the nonrelativistic Cd^{2+} and Te^{6+} pseudopotentials generated according to the Troullier-Martins[23] and Hamann[24] scheme. In order to improve the performance of the Cd pseudopotential for the simulation of CdTe surfaces, the partly ionized valence configuration $s^{1.0}p^{0.5}$ was chosen for its calculation. By doing this we expect to model the frozen core of the Cd pseudopotential and especially the $4d$ orbital in a way that makes it resemble the Cd atom in the CdTe crystal more closely. We found that the Cd pseudopotential yields the best results when the nonlocal *s* and *p* components are of the Troullier-Martins type and the local *d* component of the Hamann type. Furthermore, the nonlinear core correction[22] was applied. The Te pseudopotential was constructed entirely according to the prescription of Hamann for the s^2p^4 ground state.

The performance of these pseudopotentials was tested by simulating basic properties of CdTe bulk at a plane wave cutoff energy of 20 Ry. The equilibrium lattice constant for the zinc blende crystal was computed to be 6.54 Å, its bulk modulus 0.434 Mbar, the frequency of the TO phonon at the center of the Brillouin zone 151.6 cm^{-1}, and its cohesive energy 5.40 eV, in good overall agreement with experimentally determined values. Therefore the performance of our pseudopotentials is comparable to other pseudopotentials for Cd and Te which can be found in the literature.[25]

In order to estimate the convergence of our calculations we repeated these calculations with a cutoff energy of only 15 Ry. While the above listed CdTe bulk properties are virtually unchanged, we found that our calculated value for the heat of formation moved closer to its experimental value (see below) when the higher cutoff energy was employed. Therefore a cutoff energy of 20 Ry was finally chosen for the surface energy calculations.

For the calculation of the surface energies a slab geometry was chosen which consisted of six or seven monoatomic layers of CdTe, depending on the surface termination, and the equivalent of five or six monoatomic layers of vacuum between adjacent slabs. The lower side of the slab consisted of an unreconstructed Te-terminated surface with the dangling bonds being saturated by hydrogenlike atoms carrying a charge of $Z=0.5$, following a suggestion of Shiraishi.[26] The resulting dipole moment of the slab was compensated by a virtual dipole layer in the vacuum spacing whose magnitude was calculated self-consistently. Exchange and correlation contributions were modeled employing the LDA in the parametrization of Perdew and Zunger.[27] The scheme of Monkhorst and Pack[28] was adopted for the generation of a set of special $\vec{k}$ points, their number being equivalent to 32 per 1×1 surface cell. The positions of all atoms with the exception of those in the lowest two CdTe atomic layers were relaxed using Hellmann-Feynman forces until the magnitude of each force component was below 0.02 eV/Å. A detailed description of the program *fhi96md* that was used for this part of our calculations can be found elsewhere.[29] From simulations at different cutoff energies, we conclude that the differences in surface energies for iso stoichiometric reconstructions converged to within less than 5 meV per 1×1 surface cell.

The absolute surface energies were calculated from the total energies of the respective slabs using a scheme introduced by Qian, Martin, and Chadi.[30] In doing so, first a suitable energy was subtracted in order to account for the contribution of the hydrogenlike passivated lower side of the slab. Then the surface energy Γ was computed from the formula

$$\Gamma = E'_{\mathrm{tot}} - 0.5(n_{\mathrm{Cd}} - n_{\mathrm{Te}})\,\Delta\mu, \tag{1}$$

where

$$E'_{\mathrm{tot}} = E_{\mathrm{tot}} - 0.5\,(n_{\mathrm{Cd}} + n_{\mathrm{Te}})\,\mu^{\mathrm{bulk}}_{\mathrm{CdTe}} - 0.5\,(n_{\mathrm{Cd}} - n_{\mathrm{Te}}) \times (\mu^{\mathrm{bulk}}_{\mathrm{Cd}} - \mu^{\mathrm{bulk}}_{\mathrm{Te}}), \tag{2}$$

$$\Delta\mu = (\mu_{\mathrm{Cd}} - \mu^{\mathrm{bulk}}_{\mathrm{Cd}}) - (\mu_{\mathrm{Te}} - \mu^{\mathrm{bulk}}_{\mathrm{Te}}). \tag{3}$$

Here *n* denotes the number of atoms of the respective species within the supercell, and μ denotes the respective chemical potential. The superscript ''bulk'' refers to the chemical potential of the elementary bulk material referred to in the subscript. The chemical potentials of bulk Cd and bulk Te were calculated self-consistently by optimizing their respective supercell geometries until the minimum of the total energy was reached. Calculating from these data the heat of formation for CdTe bulk ΔH^f_0(CdTe) we found a value of -0.67 eV, which is significantly lower than the experimentally determined value of -1.05 eV.[31] In the above expression for Γ, $\Delta\mu$ extends over the interval $-\Delta H^f_0 < \Delta\mu < \Delta H^f_0$. Since this formula is symmetric with respect to the chemical potentials of the two constituents, we expect that it will minimize the error arising from the difference between the self-consistently calculated value for $\mu^{\mathrm{bulk}}_{\mathrm{CdTe}}$ and that taken from the literature.

III. STABILITY OF RECONSTRUCTIONS OF THE CdTe (001) SURFACE

Schematic ball and stick representations of the reconstructions considered in this work are shown in Fig. 1. The surface energies of these reconstructions are plotted in Fig. 2 against the variable $\Delta\mu$, as defined in Eq. (3). Enclosed

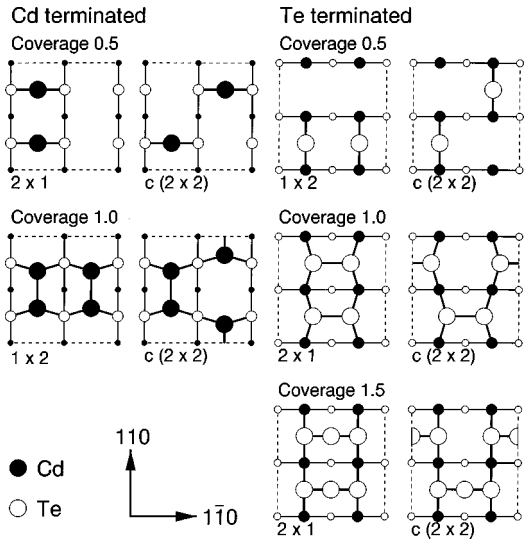

FIG. 1. Schematic ball and stick models of the surface reconstructions considered in this work.

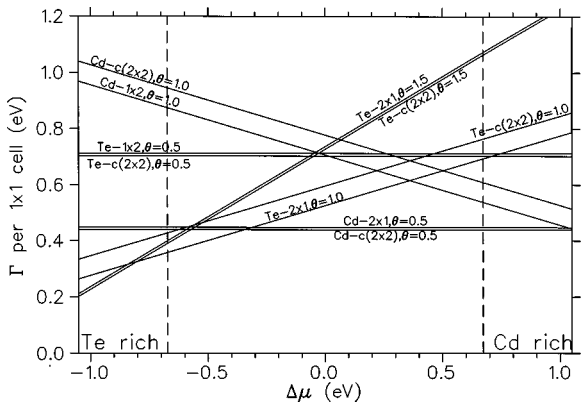

FIG. 2. Surface energies of the reconstructions from Fig. 1 plotted against the chemical potential of Te.

within the dashed lines is the interval given by the self-consistently determined value for the heat of formation of bulk CdTe. The abscissa extends towards lower values as far as -1.05 eV and to higher ones as far as 1.05 eV, the experimental value for ΔH_0^f(CdTe).

According to Eq. (1) the slopes of the lines shown in Fig. 2 represent the different stoichiometries of the respective reconstructions. The lines representing the half-covered surfaces are flat since the difference between the numbers of Cd and Te atoms per cell is zero and therefore the surface energy does not depend on the difference in the chemical potentials of the involved species.

From Fig. 2 we predict the Cd-terminated and half-covered surface to be most stable over the greater part of the range of $\Delta\mu$. Similar to the ordering observed for ZnSe the $c(2\times2)$ reconstruction is energetically favorable to the 2×1 reconstruction although the difference in surface energies is less than half that observed for ZnSe. García and Northrup[17] demonstrated that the difference in energies for the two Zn-terminated ZnSe surfaces could be explained by screening of the electrostatic repulsion between the surface Zn atoms. The increased lattice constant and higher dielectric constant of bulk CdTe with respect to ZnSe might explain at least in part the decrease in the difference in energies between the two Cd-terminated reconstructions with a coverage of $\Theta=0.5$, compared to ZnSe. The angle between the two Te—Cd bonds at the surface is about 173°, indicating that the surface Cd atoms are mainly sp hybridized. The length of the Cd—Te bond at the surface is about 6.1% shorter than in CdTe bulk, due to the rigidity of the CdTe lattice beneath the surface.

Precise atomic positions for the $c(2\times2)$ reconstructed surface have been established from a grazing incidence x-ray diffraction study conducted by Veron *et al.*[2] The positions they published are shown in Table I compared to those for the same surface that were found in our simulations. In particular, the displacements in the second atomic layer are nearly equal. The difference in the fourth layer can be attributed to the hindrance imposed in our simulations in which the atoms in the layers beneath were fixed at their ideal bulk positions. The difference in the Z positions of the surface Cd atom is significant, but since it is less tightly bound than the atoms in the layers beneath, it may be explained by a variety of reasons on the theoretical as well as the experimental side. While the vertical displacements beneath the top layer point in opposite directions, we mention that the outward displacement of these layers has also been found by García and Northrup[17] for ZnSe.

In the case of the CdTe surfaces terminated with one atomic layer of Te, the increased stability of the 2×1 reconstructed surface with respect to the $c(2\times2)$ reconstructed one has already been explained for the case of ZnSe by García and Northrup,[17] who pointed out that lateral relaxation in the second atomic layer is inhibited by the symmetry of the ZnSe surface. The energy difference of 0.07 eV per

TABLE I. Surface atomic positions given by Veron *et al.*, compared to the relaxed positions obtained from the present simulations. Coordinates are in units of $\sqrt{2}\,a_0$ on the X and Y axes and a_0 on the Z axis.

	Veron *et al.*			Present work		
	$X_0+\Delta X$	$Y_0+\Delta Y$	$Z_0+\Delta Z$	$X_0+\Delta X$	$Y_0+\Delta Y$	$Z_0+\Delta Z$
Cd 1	0.25	0	$-0.25+0.239$	0.25	0	$-0.25+0.227$
Te 2	$0.0-0.036$	0	0.0	$0.0-0.035$	0	0.0
	$0.5+0.036$	0	0.0	$0.5+0.035$	0	0.0
Cd 3	0.0	0.25	$0.25-0.005$	0.0	0.25	$0.25+0.002$
	0.5	0.25	$0.25-0.005$	0.5	0.25	$0.25+0.002$
Te 4	0.25	$0.25-0.005$	$0.5-0.008$	0.25	$0.25-0.001$	$0.5+0.005$
	0.25	$0.75+0.005$	$0.5-0.008$	0.25	$0.75+0.001$	$0.5+0.005$

1×1 surface cell between the two Te-terminated reconstructions of the CdTe surface found in this work is comparable to that published by García and Northrup for ZnSe. The Te—Te dimer length is about 2.79 Å and is almost identical with the Cd—Te bond length of 2.83 Å in CdTe bulk.

At the Cd rich limit of $\Delta\mu$, a 1×2 reconstructed CdTe surface featuring Cd dimers becomes energetically equal to the $c(2\times2)$ reconstructed surface described above. Although this value of $\Delta\mu$ is outside the range that is spanned by the self-consistently determined heat of formation for CdTe bulk, it is at the edge of the one given by the experimental value of ΔH_0^f(CdTe). Experimental evidence for a Cd rich surface has already been given by Tatarenko *et al.*,[10] who observed a $c(2\times2)$ reconstructed surface that was terminated with about 0.8 atomic layers of Cd, using x-ray photoelectron spectroscopy (XPS). It may be assumed that such a Cd rich surface consists of a mixture of the most stable reconstructions in this range of $\Delta\mu$. Consequently the reconstruction that is formed on such a mixed surface will depend on the interaction between the different terminations that are present on it.

Similar to ZnSe, where a surface covered with 1.5 atomic layers of Se is known to become stable within the allowed range of the chemical potential of Se, we find that such a Te-terminated CdTe surface should become stable at the Te rich limit of $\Delta\mu$. Such a ZnSe surface has in fact been prepared, not by epitaxial growth but by capping a ZnSe layer with Se and slowly evaporating the Se cap.[32] Therefore the formation of such a surface might also be demonstrated, though perhaps not in thermal equilibrium, within experiments aimed at the investigation of CdTe growth. Daudin, Brun-Le Cunff, and Tatarenko[14] report on atomic layer epitaxy (ALE) growth of CdTe at substrate temperatures below 24 °C where a growth rate of one monolayer per cycle was obtained. They interpret their observations by assuming the presence of a CdTe surface covered with 1.5 atomic layers of Te.

Surface reconstruction of the CdTe surface terminated with 0.5 atomic layers of Te is predicted to remain unstable over the whole range of the Te chemical potential. We found that the angle between the two Cd—Te bonds at the surface is only 76°–77° while the bond length is about 5.4% smaller than that in CdTe bulk and therefore similar to the surface bond length of the most stable Cd-terminated surfaces. Assuming the Te atoms at the surface to be sp hybridized, the expected bonding angle would be 90°. We think that the further decrease in the bonding angle is induced by the rigidity of the bonds extending from the sp^2 hybridized Cd atoms in the second layer. This explanation is supported by the observed lateral displacement of these atoms towards the top Te atoms.

IV. ELECTRONIC STRUCTURE OF THE Cd-VACANCY CdTe(001)-$c(2\times2)$ SURFACE

In this section we will present a detailed analysis of the electronic structure at the CdTe(001) surface in the $c(2\times2)$ reconstruction model. First, the results of the Kohn-Sham-LDA approach will be discussed. Next, self-energy shifts due to electron-electron interactions, calculated within the *GW* approximation, will be presented.

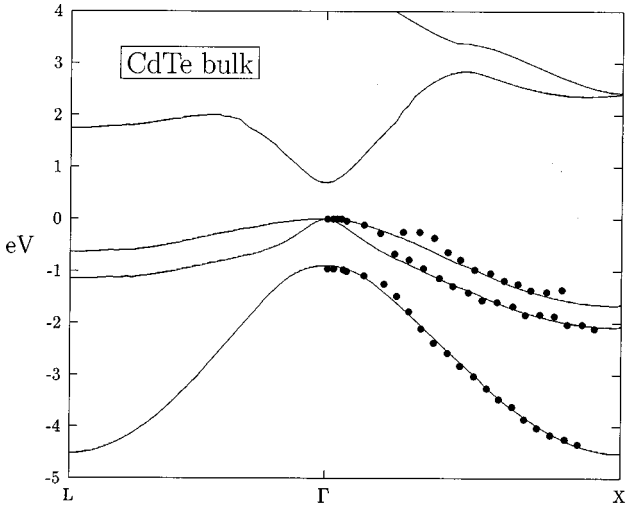

FIG. 3. Calculated bulk electronic structure of CdTe and the normal emission ARPES results of Niles and Höchst (Ref. 7) (full circles).

The calculations of this section technically differ from those of the previous one. Because of the importance of the spin-orbit interaction due to Te-5p states, we have used the relativistic Te pseudopotential from Ref. 33 and the Cd^{2+} pseudopotential with the partial core charge correction from Ref. 25, whose analytical form is similar. Figure 3 shows a portion of the bulk band structure of CdTe along ΓX and ΓL directions obtained with these pseudopotentials at the experimental lattice constant. The full circles denote the experimentally determined dispersion of occupied bands along ΓX.[7] The agreement with photoemission measurements of Niles and Höchst is excellent. Another technical difference from the preceding section is the construction of the periodic slab. Here we do not cover one surface of the slab with hydrogen atoms, but instead use symmetric slabs. Such a geometry introduces an artificial interaction of surface states across the slab. In order to minimize this effect we have used larger slabs, which in the case of the LDA calculation contained 21 atomic layers. The resulting energy splitting of bonding-antibonding combinations of surface states from opposite surfaces was smaller than 0.04 eV. In the same time we have relaxed the cutoff limit for plane waves to 10 Ry. The energy shift of the bulk band structure caused by this reduction of the cutoff was on average smaller than 0.08 eV. The atomic positions of the uppermost three layers have been assigned to the values calculated in the preceding section. We have determined the binding energies of surface states and resonances from a comparison of the local density of states at the surface with that of the bulk and from an inspection of the spatial behavior of the Kohn-Sham wave functions. The results are presented within the Brillouin zone for the unreconstructed 1×1 surface. We first present results of the LDA calculation.

A. LDA calculation

For the Cd-vacancy $c(2\times2)$ structure there are half as many Cd atoms at the surface as in a regular Cd atomic layer. Each surface Cd atom provides two electrons. The Cd-vacancy structure permits redistribution of these two

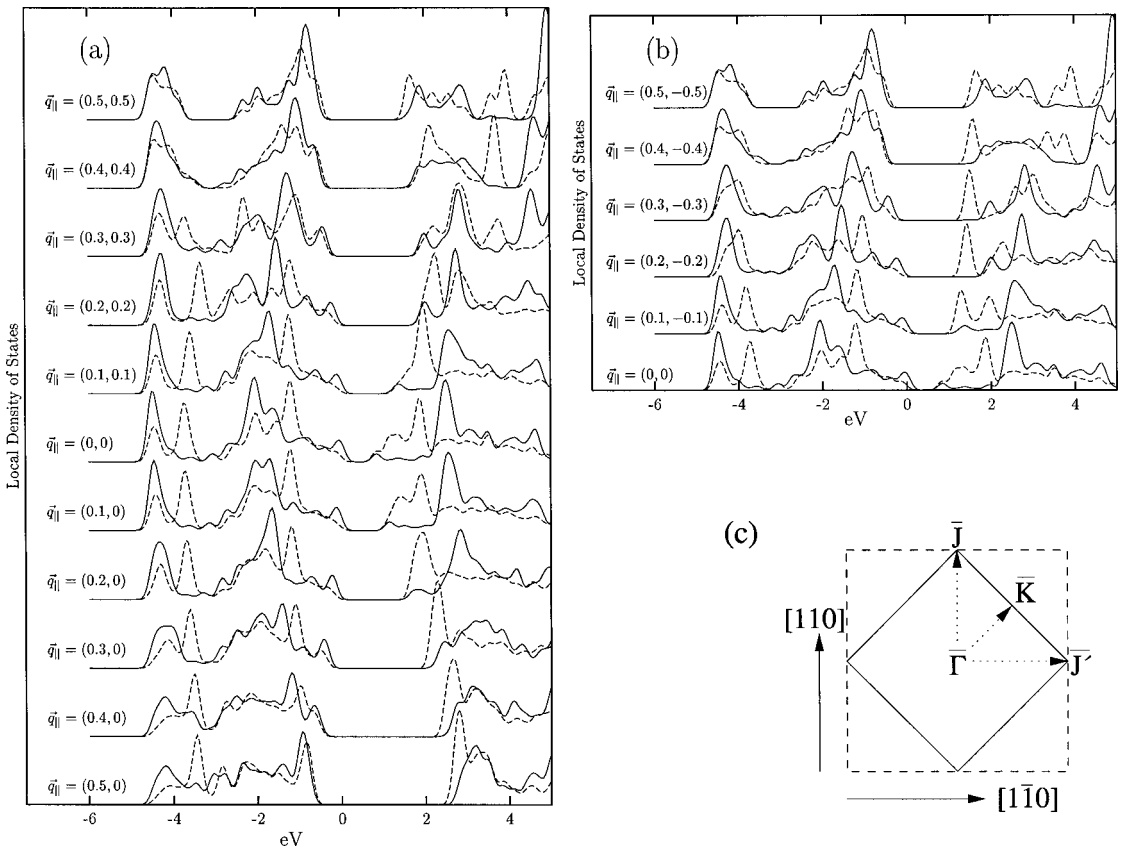

FIG. 4. Local density of states calculated in the central layer (solid line) and the surface layer (dashed line) of the 21 atomic layer thick slab for CdTe(001)-$c(2\times2)$ Cd-vacancy type reconstruction. (a) shows the dispersion of LDOS along the $\overline{J\Gamma K}$ direction and (b) along the $\overline{J'\Gamma}$ direction. $\vec{q}_\parallel$ is given in $2\pi/a$ units, with $a=12.245$ a.u. (c) shows the $c(2\times2)$ Brillouin zone. The symbols $\bar{\Gamma}, \bar{J}, \bar{J}'$, and $\bar{K}$ are defined in the text.

electrons such that the dangling anion (Te) bonds are fully occupied and the cation (Cd) dangling bonds fully empty, thus leading to a semiconducting energy structure.

Figures 4(a) and 4(b) show the dispersion of the local density of states (LDOS) computed at the central layers of the slab (solid line) and at the surface layer (dashed line) along three crystallographic directions. Alternatively, the solid lines could be obtained by superimposing the bulk LDOS for two different $q_\parallel$ vectors shifted by $\vec{G}_\parallel=(2\pi/a)\times(1,0)$. Figure 4 (c) presents the $c(2\times2)$ surface Brillouin zone and the symmetry directions along which the electronic structure is analyzed. Since the LDOS has been calculated with an energy broadening of 0.15 eV, the sharp structures in LDOS have been smoothed. LDOS from 6 eV below the valence band maximum (VBM) to 4 eV above are shown. The lower-energy region, containing the Te-5s and Cd-4d states, is not properly described by our calculation, due to the lack of Cd-4d states. It is also not covered by the published angular-resolved photoemission results of Niles and Höchst[7] and Gawlik *et al.*[8,9]

The dashed lines in Figs. 4(a) and 4(b) show distinct peaks caused by the presence of surface states and resonances. An inspection of the spatial behavior of the Kohn-Sham orbitals in these energy regions confirms the surface character of these states. In Figs. 5(a) and 6(a) the planar average of two occupied orbitals at the center of two surface peaks in LDOS at $q_\parallel=0$ is shown. Figures 5(b) and 6(b) give contour plots for these orbitals. The results shown in Fig. 4 together with a detailed analysis of the spatial character of each orbital allow a determination of the surface band structure for the $c(2\times2)$ reconstruction model. Full circles in Fig. 7 show surface features (surface states and resonances) along the $\overline{J\Gamma K}$ line obtained in this way. Open circles give the results for the $\overline{J'\Gamma}$ line. The symbols denote the following points in the surface Brillouin zone: $\bar{\Gamma}=(0,0)$, $\bar{K}=(2\pi/a)(1,0)$, $\bar{J}=(2\pi/a)(\frac{1}{2},\frac{1}{2})$, and $\bar{J}'=(2\pi/a)(\frac{1}{2},-\frac{1}{2})$, where a is the cubic lattice constant. For the (001) surface of the zinc blende symmetry materials the directions $\overline{J\Gamma}$ and $\overline{J'\Gamma}$ are not equivalent, therefore, the surface structure at both lines is different. We show the results on top of the surface projected bulk band structure (shadowed regions of Fig. 7) for the unreconstructed surface. Because the $c(2\times2)$ reconstruction has a double periodicity in the [1,0] direction, the actual border of the $c(2\times2)$ Brillouin zone is at the $(2\pi/a)(\frac{1}{2},0)$ point, which is represented by a vertical dotted line.

There are two main occupied surface resonances visible in Fig. 7. Both exhibit a rather small dispersion along the $\overline{\Gamma K}$ direction and a more pronounced dispersion along the $\overline{\Gamma J}$ and $\overline{\Gamma J'}$ lines. The binding energy at the center of the lower resonance at the $\bar{\Gamma}$ point is 3.74 eV and of the upper reso-

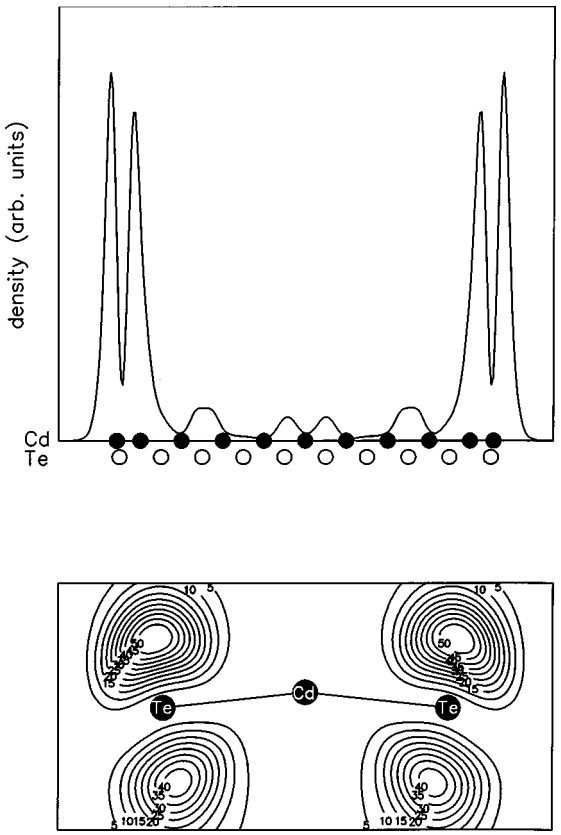

FIG. 5. (a) Surface normal dependence of the planar average of the modulus square of the wave function of the occupied dangling bond surface resonance at -1.22 eV at the $\overline{\Gamma}$ point. Full circles show the position of Cd atomic layers, empty circles of the Te atomic layers. (b) Contour plot in the Cd-Te plane for this orbital.

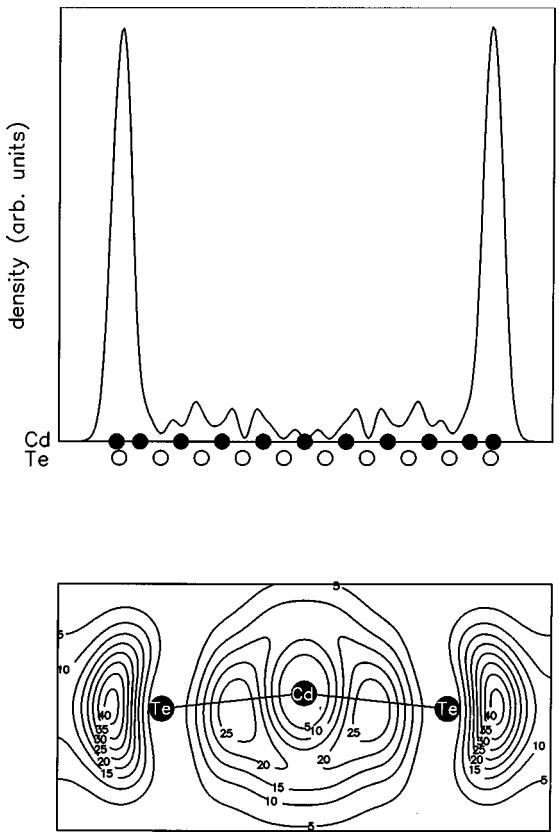

FIG. 6. Same as in Fig. 5 for the occupied backbond surface resonance at -3.74 eV at the $\overline{\Gamma}$ point.

nance is 1.22 eV with respect to the valence band maximum. An analysis of the spatial character of the wave functions reveals that the upper band at -1.22 eV is built from occupied dangling bonds on the subsurface Te atoms [Fig. 5(b)]. The angle between the Te—Cd bond and the dangling bond is close to 90°. The lower resonance at -3.74 eV is formed by the bonding states between the surface Cd atoms and the subsurface, neighboring Te atoms. As was pointed out in the preceding section, the Cd-Te distance is shorter for surface atoms compared with the bulk atoms, which favors a stronger binding of these states.

Our LDA calculation places the vacuum level at 4.9 eV above the valence band maximum. There are two branches of unoccupied dispersive resonances below the vacuum level. They form true surface states in the large energy gap along the $\overline{\Gamma J}$, $\overline{\Gamma J'}$ directions and a rather flat surface state below the projected bulk bands in the $\overline{\Gamma J'}$ direction.

Finally we note that the configuration of occupied and empty surface states would not favor the formation of a surface charge layer[34] at the CdTe(001)-$c(2\times2)$ surface and this surface should remain neutral. Consistent with this conclusion, the existence of surface charges and the resulting band bending has not been experimentally reported.

B. *GW* calculation

It is a well known fact that the Kohn-Sham one-electron energies do not, formally, represent the energies of one-particle excitations in a many-electron system, e.g., the band structure of a solid measured in the photoemission experiments. Nevertheless, it is also well known that for weakly correlated materials, apart from the gap problem, the Kohn-Sham energy bands agree rather well with experimental measurements. This is also documented by the good agreement

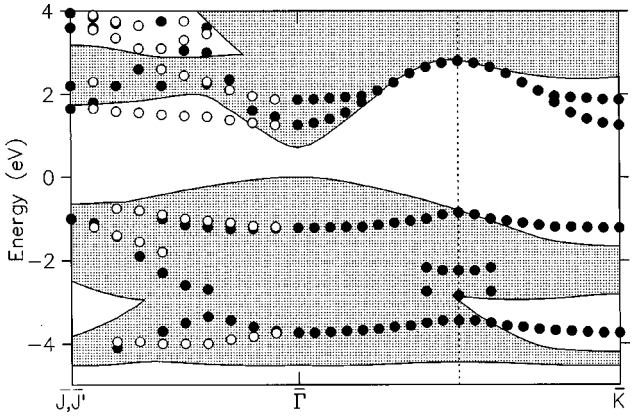

FIG. 7. Electronic structure for the CdTe(001)-$c(2\times2)$ Cd-vacancy surface shown within the unreconstructed (1×1) Brillouin zone. Full and empty circles give the positions of the surface states and resonances obtained within the LDA approximation for the 21 atomic layer thick slab. Full circles: surface features along the $\overline{J\Gamma K}$ direction. Empty circles: along the $\overline{J'\Gamma}$ direction. The vertical dotted line denotes the border of the $c(2\times2)$ Brillouin zone in the (1,0) direction. The symbols $\overline{\Gamma}$,$\overline{J}$,$\overline{J'}$, and $\overline{K}$ are defined in the text.

of the LDA bulk valence bands with the experimental photoemission spectrum as seen in Fig. 3. However, an interesting and important question is whether the same holds for surface states and resonances. There is no *a priori* obvious answer to this question, because in the surface region several factors, such as a sharp change in the electron density, its smaller values, and the localization of the electron states, could lead to the enhancement of correlation effects. A few existing calculations of many-body shifts of surface states in semiconductors show certain effects, whose understanding and the possible prediction of systematic trends has not yet been fully achieved. Motivated by this lack we have done an explicit calculation of the self-energy within the *GW* approximation for the $c(2\times2)$ Cd-vacancy structure.

We shall not describe here details of the *GW* method but instead refer the interested reader to two very recent reviews.[35,36] Briefly, we have calculated the *static* dielectric matrix for a uniform mesh of $\vec{k}$ points within the surface Brillouin zone[37] and have applied the so-called plasmon-pole approximation[38,39] in order to model the energy dependence of the screening. Because *GW* calculations are numerically complex and the computational requirements increase extremely fast with the increasing system size, the number of atomic layers in the $c(2\times2)$ slab was reduced to nine (from 21 with which the LDA electronic structure in Figs. 4–7 was calculated). The cutoff for screening matrices in Fourier space was set to 5 Ry. We stress here the importance of the consideration of the full matrix character of the response functions, because the site dependence of screening is contained in their off-diagonal matrix elements. An important point in the analysis of the results of a *GW* calculation done for the slab geometry is a proper assignment of energy shifts of surface features. The problem arrises from the small size of slabs used, which together with the higher sensitivity of the *nonlocal* self-energy operator to the more distant space regions, compared to the LDA exchange-correlation potential, leads to convergence difficulties in the precise reproduction of the bulk electronic structure in the central region of the slab. This problem was discussed by Hybertsen and Louie in Ref. 41. Following a suggestion of these authors, we have determined the self-energy shifts of surface features by comparing their relative shifts (in the *GW* and LDA calculations) with respect to main bulk peaks in the one dimensional ($\vec{k}_\parallel$-resolved) local density of states. The self-energy shifts of surface states and resonances obtained in this manner have been added to the LDA positions of these states shown in Fig. 7 and the results are presented in Fig. 8 (big filled circles). We consider here only the occupied part of the spectrum. As was shown for CdS in Ref. 40 and also confirmed by our calculation, the use of a Cd^{2+} pseudopotential results in an absolute energy gap which is too large. For the bulk energy gap of CdTe we obtain a value which is 0.7 eV larger than the experimental one. Our opinion is that this overestimation is connected to the absence of semicore Cd-4*d* states, whose presence, as well as that of other core states from the Cd $n=4$ shell,[40] is necessary for a correct description of the energy gap in cadmium chalcogenides.

The big filled circles in Fig. 8 indicate the binding energies of occupied surface features along the $\overline{K\Gamma K}$ line, calculated within the *GW* approximation. The small filled circles

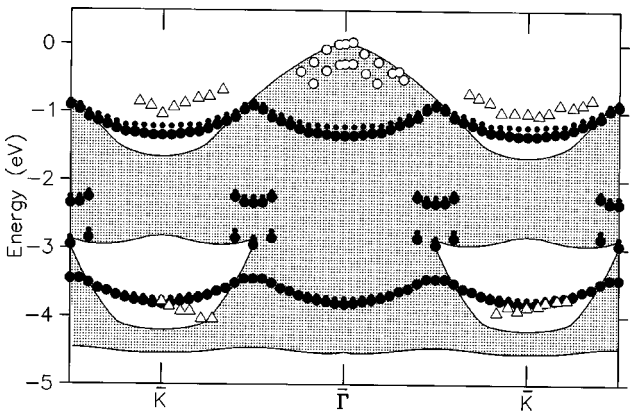

FIG. 8. Electronic structure for the CdTe(001)-$c(2\times2)$ Cd-vacancy surface calculated within the LDA (small full circles) and the GW (big full circles) approximations. Empty triangles and circles: ARPES results of Ref. 8.

represent the LDA results, shown previously in Fig. 7. It is noteworthy that the effect of many-body interactions on the LDA surface features is clearly a shift towards higher binding energies. This shift is $\vec{k}_\parallel$ dependent, contributing to the slightly enhanced dispersion of occupied surface bands. Values of the self-energy shifts range between 0 and 0.2 eV. This result is in agreement with basically all previously published *GW* calculations for semiconductor surfaces,[41,42] where a rather pronounced negative shift of occupied surface features is reported, with the exception of the Si(001)-(2 $\times1$) and Ge(001)-(2×1) (Ref. 43) surfaces. It is interesting to note that the self-energy shifts are slightly bigger for the dangling bond states on the subsurface Te atoms (Fig. 5) than for the backbond states (Fig. 6).

C. Comparison with experiment

We are aware of three angle-resolved photoelectron spectroscopy (ARPES) measurements of the electronic structure of the CdTe(001) surface, with which our calculations could be compared. Niles and Höchst[7] have reported normal emission ARPES done on the CdTe(001)-(1×2) surface. Gawlik *et al.*[8] have presented the results of an ARPES study of the unreconstructed CdTe(001)-(1×1) surface. In a following article by the same group,[9] normal emission spectra for the CdTe(001)-$c(2\times2)$ surface have been given. None of the above articles makes a definitive statement about the termination and stoichiometry of the surface. Whereas the work of Niles and Höchst is focused on dispersive photoemission structures, which correspond to bulk transitions, both studies of Gawlik *et al.* give information about possible surface features. For the unreconstructed (1×1) surface, Gawlik *et al.*[8] report off-normal emission spectra, resulting in a surface electronic structure along the $\overline{\Gamma K}$ line.

Simple considerations based on the electron counting rule[44] exclude the unreconstructed and clean CdTe(001)-(1 $\times1$) surface from the set of stable structures. However, no metallic behavior and a clear energy gap is seen in the ARPES spectra of Ref. 8. Therefore, it is very likely that the apparently (1×1) unreconstructed surface was a result of disorder and the small size of domains possessing an ''allowed'' reconstruction pattern. A typical low-energy electron

diffraction (LEED) picture of the CdTe(001)-$c(2\times2)$ surface shows a stronger (1×1) pattern and a weaker $c(2\times2)$ superstructure,[6] which is consistent with the pronounced relaxation of the surface Cd atoms towards the subsurface Te plane. It is also known that the (1×1) LEED patterns seen sometimes on the CdTe(001) surfaces are never sharp and clean, which complies well with the conjecture that they originate from a surface disorder.[45] We shall assume that the ARPES spectra presented in Refs. 8 and 9 are due to the $c(2\times2)$ Cd-vacancy structure and compare them with our results.

The empty triangles in Fig. 8 represent distinct surface features identified by Gawlik *et al.*[8] in the ARPES spectra. The agreement between our calculations and the ARPES experiment is rather remarkable for the surface states with a binding energy of about 3.9 eV, which are located in the open pocket of the projected bulk bands close to the $\bar{K}$ point. The agreement is also satisfactory for the surface states above the upper bulk edge near the $\bar{K}$ point, although here the calculations clearly give lower-energy positions. For these states, the *GW* approximation shifts the LDA results further away from the experimental results. An open question remains as to whether this effect comes from the convergence requirements of the *GW* method (slab size, sampling-$\vec{k}$ mesh, etc.), or from the surface disorder and preparations of experimental samples. It is understandable that both surface bands show up in the ARPES experiment around the $\bar{K}$ point and not near the $\bar{\Gamma}$ point, although in the $c(2\times2)$ structure both points are equivalent and the calculated surface electronic structure is $\bar{\Gamma}\bar{K}$ periodic. As we have explicitly checked, for both surface states at $\bar{\Gamma}$, the $\vec{k}_{\bar{K}}+\vec{G}$ coefficients of the Fourier expansion of wave functions strongly dominate over the $\vec{G}$ coefficients, where the $\vec{G}$ vectors are the reciprocal-lattice vectors for the unreconstructed (1×1) surface. Such wave functions couple more strongly to outgoing plane waves with off-normal, $\vec{k}=\vec{k}_{\bar{K}}$ vector.

The empty circles in Fig. 8 indicate the positions of those ARPES features for which the evidence of their surface character is not as strong because of the presence of bulk transitions in their vicinity. These states are not present in our calculation.[46] Whereas the experimental evidence of the surface character of these states is rather weak, the assignment of the empty circles to surface resonances in Ref. 8 was based on a calculation of a Cd-terminated and *unreconstructed* CdTe(001)-(1×1) surface, which predicted surface resonances in that energy region. Our results do not confirm this conclusion. On the other hand, the energy positions of the empty circles at $\bar{\Gamma}$ agree well with the S_1 and S_2 features in the normal emission ARPES results for the CdTe(001)-$c(2\times2)$ surface reported later by the same group (Fig. 1 in Ref. 9). The assignment of an ARPES peak as a surface structure relies on the stationary peak position with respect to the photon energy. However, as has been recently shown by an analysis of ARPES spectra of BeTe,[47] such stationary peaks occur close to the valence band maximum, which do not originate from a surface state, but rather from a pronounced lifetime broadening of the final photoemission states. We suggest that at least the S_1 peak in Fig. 1 of Ref. 9 has a similar character.

The S_3, S_4, and S_5 surface ARPES features seen in the same normal emission spectra for the CdTe(001)-$c(2\times2)$ surface are very close to the positions of the empty triangles in the open pocket of the projected bulk states in Fig. 8 and to our lower surface band. Thus it appears that the existence of this surface band is experimentally well established. As far as the upper surface band is concerned, the authors of Ref. 9 do not assign a surface feature at the energy range about -1 eV below the VBM in their ARPES spectra for CdTe(001)-$c(2\times2)$. However, there seems to be present in their Fig. 1 a nondispersive broad peak at this energy, which appears when the photon energy enters the surface-sensitive range of energies ($\hbar\omega>20$ eV).

There is another nondispersive feature present in basically all ARPES spectra for various CdTe surfaces and for other materials as well. This is a broad peak at the lower edge of the valence band placed at -4.4 eV in Ref. 7 and at -4.7 eV in Ref. 9. This photoemission structure is sometimes interpreted as a surface feature and sometimes as a bulk feature due to indirect transitions from the high density of states region around the critical points in the band structure. The authors of both ARPES studies[7,9] favor the latter interpretation. Our calculations, in which no surface feature is found at the lower edge of the valence band, seem to corroborate the latter interpretation as well.

V. SUMMARY

The CdTe(001) surface has been studied theoretically within the LDA and *GW* methods. In the first step, atomic geometries of various reconstruction models have been optimized by means of total energy and force calculations. A phase diagram of stable structures has been determined. It was shown that over a broad range of ambient conditions the $c(2\times2)$ Cd-vacancy reconstruction model with a strong relaxation of surface Cd atoms in the direction of the bulk is the most stable structure. In the second part of the article the electronic structure at the $c(2\times2)$ surface has been obtained and analyzed in detail. We have found basically two occupied surface bands, which show up as distinct peaks in the local density of state curves calculated within the LDA approximation for very large slabs. Many-body interactions obtained within the *GW* approximation shift these surface resonances slightly downward. Our theoretical electronic structure has been compared to angle-resolved photoemission measurements and agrees rather well with these and other published experiments. At some points, our results seem to suggest a new interpretation of the experimental data. We hope to motivate future angular-resolved photoemission measurements on high-quality samples with well defined surface geometry.

ACKNOWLEDGMENTS

We thank C. R. Becker for reading the manuscript, and for his comments and suggestions. We also thank P. Hawrylak for useful discussions. This work was financially supported by the Deutsche Forschungsgemeinschaft under Project No. SFB 410. Part of the calculations have been performed at the Leibnitz Rechenzentrum in Munich.

[1] L. Seehofer, G. Falkenberg, R.L. Johnson, V.H. Etgens, S. Tatarenko, D. Brun, and B. Daudin, Appl. Phys. Lett. **67**, 1680 (1995); L. Seehofer, V.H. Etgens, G. Falkenberg, M.B. Veron, D. Brun, B. Daudin, S. Tatarenko, and R.L. Johnson, Surf. Sci. **347**, L55 (1996).

[2] M.B. Veron, M. Sauvage-Simkin, V.H. Etgens, S. Tatarenko, H.A. Van Der Vegt, and S. Ferrer, Appl. Phys. Lett. **67**, 3957 (1995); M.B. Veron, V.H. Etgens, M. Sauvage-Simkin, S. Tatarenko, B. Daudin, and D. Brun-Le Cunff, J. Cryst. Growth **159**, 694 (1996).

[3] Y.S. Wu, C.R. Becker, A. Waag, M.M. Kraus, R.N. Bicknell-Tassius, and G. Landwehr, Phys. Rev. B **44**, 8904 (1991).

[4] S. Tatarenko, B. Daudin, D. Brun, V.H. Etgens, and M.B. Veron, Phys. Rev. B **50**, 18 479 (1994).

[5] P. Lu and D.J. Smith, Surf. Sci. **254**, 119 (1991).

[6] H. Neureiter, S. Spranger, M. Schneider, U. Winkler, M. Sokolowski, and E. Umbach, Surf. Sci. **388**, 186 (1997).

[7] D.W. Niles and H. Höchst, Phys. Rev. B **43**, 1492 (1991).

[8] K.-U. Gawlik, J. Brügmann, S. Harm, C. Janowitz, R. Manzke, M. Skibowski, C.-H. Solterbeck, W. Schattke, and B. A. Orłowski, in *The Physics of Semiconductors, Proceedings of the 21st International Conference*, edited by Ping Jiang and Hou-Zhi Zheng (World Scientific, Singapore, 1992), p. 485; Acta Phys. Pol. A **82**, 355 (1992).

[9] K.-U. Gawlik, J. Brügmann, S. Harm, R. Manzke, M. Skibowski, B.J. Kowalski, and B.A. Orlowski, Acta Phys. Pol. A **84**, 1093 (1993).

[10] S. Tatarenko, F. Bassani, J.C. Klein, K. Saminadayar, J. Cibert, and V.H. Etgens, J. Vac. Sci. Technol. A **12**, 140 (1994).

[11] W. Chen, A. Kahn, P. Soukiassian, P.S. Mangat, J. Gaine, C. Ponzoni, and D. Olego, Phys. Rev. B **49**, 10 790 (1994); J. Vac. Sci. Technol. B **12**, 2639 (1994).

[12] C. Heske, U. Winkler, H. Neureiter, M. Sokolowski, R. Fink, E. Umbach, Ch. Jung, and P.R. Bressler, Appl. Phys. Lett. **70**, 1022 (1997); C. Heske, U. Winkler, G. Held, R. Fink, E. Umbach, Ch. Jung, P.R. Bressler, and Ch. Hellwig, Phys. Rev. B **56**, 2070 (1997).

[13] H. Dröge, A. Fleszar, and H.-P. Steinrück, J. Cryst. Growth **184/185**, 208 (1998).

[14] B. Daudin, D. Brun-Le Cunff, and S. Tatarenko, Surf. Sci. **352-354**, 99 (1996).

[15] K. Menda, T. Ninato, and M. Kawashima, Jpn. J. Appl. Phys., Part 1 **28**, 1560 (1989).

[16] H.H. Farrell, M.C. Tamargo, and S.M. Shibli, J. Vac. Sci. Technol. B **8**, 884 (1990).

[17] A. García and J.E. Northrup, Appl. Phys. Lett. **65**, 708 (1994); J. Vac. Sci. Technol. B **12**, 2678 (1994).

[18] C.H. Park and D.J. Chadi, Phys. Rev. B **49**, 16 467 (1994).

[19] R. Car and M. Parrinello, Phys. Rev. Lett. **55**, 2471 (1985).

[20] P. Hohenberg and W. Kohn, Phys. Rev. **136**, B864 (1965); W. Kohn and L.J. Sham, Phys. Rev. **140**, A1133 (1965).

[21] S.-H. Wei and A. Zunger, Phys. Rev. B **37**, 8958 (1988).

[22] S.G. Louie, S. Froyen, and M.L. Cohen, Phys. Rev. B **26**, 1738 (1982).

[23] N. Troullier and J.L. Martins, Phys. Rev. B **43**, 1993 (1991).

[24] D.R. Hamann, Phys. Rev. B **40**, 2980 (1989).

[25] A. Dal Corso, S. Baroni, R. Resta, and S. de Gironcoli, Phys. Rev. B **47**, 3588 (1993).

[26] K. Shiraishi, J. Phys. Soc. Jpn. **59**, 3455 (1990).

[27] We have used the parametrization by P. Perdew and A. Zunger, Phys. Rev. B **23**, 5048 (1981), of the results of D.M. Ceperley and B.I. Alder, Phys. Rev. Lett. **45**, 566 (1980).

[28] H.D. Monkhorst and J.D. Pack, Phys. Rev. B **13**, 5188 (1976).

[29] M. Bockstedte, A. Kley, J. Neugebauer, and M. Scheffler, Comput. Phys. Commun. **107**, 187 (1997).

[30] G.-X. Qian, R.M. Martin, and D.J. Chadi, Phys. Rev. B **38**, 7649 (1988).

[31] *Semiconductors: Technology of III-V, II-VI and Non-Tetrahedrally Bonded Compounds*, edited by O. Madelung, Landolt-Börnstein, New Series, Group III, Vol. 17, Pt. d (Springer, Berlin, 1982).

[32] J.-T. Zettler, K. Stahrenberg, W. Richter, H. Wenisch, B. Jobst, and D. Hommel, J. Vac. Sci. Technol. B **14**, 2757 (1996).

[33] G.B. Bachelet, D.R. Hamann, and M. Schlüter, Phys. Rev. B **26**, 4199 (1982).

[34] W. Mönch, in *Semiconductor Surfaces and Interfaces*, edited by G. Ertl, Springer Series in Surface Sciences Vol. 26, 2nd ed. (Springer, Berlin, 1995).

[35] F. Aryasetiawan and O. Gunnarsson, Rep. Prog. Phys. **61**, 237 (1998).

[36] W. G. Aulbur, L. Jönsson, and J. W. Wilkins, Solid State Phys. (to be published).

[37] Four $\vec{k}$ points of the type $(2\pi/a)(\pm\frac{1}{4},\pm\frac{1}{4},0)$ together with the $\bar{\Gamma}$ point have been used applying a surface-adapted version of the singular-$\vec{k}$ integration of F. Gygi and A. Baldereschi, Phys. Rev. B **34**, 4405 (1986).

[38] W. von der Linden and P. Horsch, Phys. Rev. B **37**, 8351 (1988).

[39] M. Rohlfing, P. Krüger, and J. Pollmann, Phys. Rev. B **48**, 17 791 (1993).

[40] M. Rohlfing, P. Krüger, and J. Pollmann, Phys. Rev. Lett. **75**, 3489 (1995).

[41] M.S. Hybertsen and S.G. Louie, Phys. Rev. B **38**, 4033 (1988).

[42] X. Zhu, S.B. Zhang, S.G. Louie, and M.L. Cohen, Phys. Rev. Lett. **63**, 2112 (1989); X. Zhu and S.G. Louie, Phys. Rev. B **43**, 12 146 (1991); J.E. Northrup, *ibid.* **47**, 10 032 (1993); X. Blase, X. Zhu, and S.G. Louie, *ibid.* **49**, 4973 (1994); C. Kress, M. Fiedler, W.G. Schmidt, and F. Bechstedt, Surf. Sci. **331-333**, 1152 (1995).

[43] M. Rohlfing, P. Krüger, and J. Pollmann, Phys. Rev. B **52**, 1905 (1995); **54**, 13 759 (1996).

[44] M.D. Pashley, Phys. Rev. B **40**, 10 481 (1989).

[45] M. Sokolowski (private communication).

[46] As a matter of fact, the surface LDOS (dashed curve in Fig. 4) close to the $\bar{\Gamma}$ point slightly dominates the bulk LDOS around -0.5 eV below the VBM. However, the effect is so small as compared with surface peaks at -3.74 eV and -1.22 eV that we do not consider these states as surface states.

[47] M. Nagelstraßer, H. Dröge, H.-P. Steinrück, F. Fischer, T. Litz, A. Waag, G. Landwehr, A. Fleszar, and W. Hanke, Phys. Rev. B **58**, 10 394 (1998).